Available online at www.sciencedirect.com
ScienceDirect
Journal of Power Sources 168 (2007) 330–337
JOURNAL OF POWER SOURCES
www.elsevier.com/locate/jpowsour

$Ba_{0.5}Sr_{0.5}Co_{0.8}Fe_{0.2}O_{3-\delta}$ + $LaCoO_3$ composite cathode for $Sm_{0.2}Ce_{0.8}O_{1.9}$-electrolyte based intermediate-temperature solid-oxide fuel cells

Wei Zhou, Zongping Shao *, Ran Ran, Pingying Zeng, Hongxia Gu, Wanqin Jin, Nanping Xu

College of Chemistry and Chemical Engineering, Nanjing University of Technology, No. 5 Xin Mofan Road, Nanjing, 210009 Jiangsu, PR China

Received 12 January 2007; received in revised form 15 March 2007; accepted 15 March 2007
Available online 24 March 2007

Abstract

A novel $Ba_{0.5}Sr_{0.5}Co_{0.8}Fe_{0.2}O_{3-\delta}$ + $LaCoO_3$ (BSCF + LC) composite oxide was investigated for the potential application as a cathode for intermediate-temperature solid-oxide fuel cells based on a $Sm_{0.2}Ce_{0.8}O_{1.9}$ (SDC) electrolyte. The LC oxide was added to BSCF cathode in order to improve its electrical conductivity. X-ray diffraction examination demonstrated that the solid-state reaction between LC and BSCF phases occurred at temperatures above 950 °C and formed the final product with the composition: $La_{0.316}Ba_{0.342}Sr_{0.342}Co_{0.863}Fe_{0.137}O_{3-\delta}$ at 1100 °C. The inter-diffusion between BSCF and LC was identified by the environmental scanning electron microscopy and energy dispersive X-ray examination. The electrical conductivity of the BSCF + LC composite oxide increased with increasing calcination temperature, and reached a maximum value of ~300 S cm^{-1} at a calcination temperature of 1050 °C, while the electrical conductivity of the pure BSCF was only ~40 S cm^{-1}. The improved conductivity resulted in attractive cathode performance. An area-specific resistance as low as 0.21 Ω cm^2 was achieved at 600 °C for the BSCF (70 vol.%) + LC (30 vol.%) composite cathode calcined at 950 °C for 5 h. Peak power densities as high as ~700 mW cm^{-2} at 650 °C and ~525 mW cm^{-2} at 600 °C were reached for the thin-film fuel cells with the optimized cathode composition and calcination temperatures.

Keywords: Solid-oxide fuel cells; Composite cathode; $Ba_{0.5}Sr_{0.5}Co_{0.8}Fe_{0.2}O_{3-\delta}$; $LaCoO_3$; Electrochemical impedance spectra

1. Introduction

Fuel cells efficiently convert chemical energy to electricity in a silent and environmentally friendly way. They are believed to be a promising alternative power source to traditional mobile and stationary sources, such as the internal combustion engine and coal burning power plants. Among the various kinds of fuel cells, solid-oxide fuel cells (SOFCs) have the benefits of the high energy efficiency and fuel flexibility because of their high operating temperature. Therefore, they have received considerable attention in recent years.

Typical SOFCs are based on the yttira-stabilized zirconia (YSZ) electrolyte and operate at ~1000 °C [1]. Such a high operating temperature is beneficial for accelerating the electrode reactions. However, it also introduces several serious problems or drawbacks, such as an interfacial reaction between the electrode and electrolyte to form insulating phase(s), the densification of the electrode layer due to high-temperature sintering, possible crack formation due to the mismatch of thermal expansion coefficient (TEC) of the cell components and the requirement of high-cost La(Ca)CrO_3 as the interconnect material [2]. The decrease of operating temperature would result in reducing reactivity between the cell components and therefore an improvement of fuel cell stability. Furthermore, much cheaper metallic interconnects and more flexible glass gasket sealants may be applied [3,4]. Therefore, there is a general tendency for SOFCs towards a reduced operating temperature (<800 °C) [5–9]. However, the decrease of operating temperature leads to a significant decrease in electrode activity, especially for the cathode [10–13]. As a result, the conventional SOFC cathode,

* Corresponding author. Tel.: +86 25 83587722.
E-mail address: shaozp@njut.edu.cn (Z. Shao).

0378-7753/$ – see front matter © 2007 Elsevier B.V. All rights reserved.
doi:10.1016/j.jpowsour.2007.03.041

strontium-doped lanthanum manganite (LSM), is not suitable for intermediate-temperature solid-oxide fuel cells (IT-SOFCs) due to its low activity below 800 °C.

Nowadays, there are growing interests in developing an improved performance cathode for IT-SOFCs [14–20]. Promising candidates are normally based on the mixed oxygen ionic and electronic conducting oxides, such as $Sm_{0.5}Sr_{0.5}CoO_{3-\delta}$ (SSC) and $La_{0.6}Sr_{0.4}Co_{0.2}Fe_{0.8}O_{3-\delta}$ (LSCF) [21–25]. The mixed conductivity extends the active oxygen reduction site from the typical electrolyte-electrode-gas triple-phase boundary to the entire exposed cathode surface, therefore greatly reducing the cathode polarization at low operating temperatures. Very recently, Shao and Haile [26] reported a mixed conducting $Ba_{0.5}Sr_{0.5}Co_{0.8}Fe_{0.2}O_{3-\delta}$ (BSCF) oxide as a potential cathode material for $Sm_{0.2}Ce_{0.8}O_{1.9}$ (SDC)-electrolyte based IT-SOFCs. The application of BSCF as a cathode material has attracted a lot of attention [27–31]. Although very promising results were reported, some disadvantages of the BSCF cathode may include the high TEC and the low electrical conductivity. A TEC as large as 21–24 $\times 10^{-6}$ K^{-1} and a conductivity of only 40–60 S cm^{-1} under air is reported [32,33]. A high electrical conductivity is important for the efficient current collection and the decrease of ohmic polarization resistance, while the correct TEC of the cathode is also important for compatibility with the electrolyte. Mixed conducting oxides usually have a higher TEC than the electrolyte. The strategy of using a composite oxide by mixing it with a second phase is frequently applied to reduce the TEC and increase the cathode performance of the SSC and LSCF cathodes, such as SSC + SDC and LSCF + $Gd_{0.2}Ce_{0.8}O_{1.9}$ (GDC) [13,34]. The performance of the BSCF + SDC has also been reported recently [26,31]. However, no significant improvement in fuel cell performance was observed, because BSCF by itself is a high oxygen ionic conductor. This is very different from the cases of the SSC or LSCF based cathodes [13,26,34]. Furthermore, the electrical conductivity decreased with the formation of a BSCF + SDC composite oxide due to the pure ionic conductivity of the SDC. An increase of the ohmic polarization from the cathode layer and the decrease of current collecting efficiency may be experienced for the BSCF + SDC cathode.

In this study, $LaCoO_3$ (LC), a high electrical conducting oxide with a reported electrical conductivity as high as 1000 S cm^{-1} [35], was investigated as the second phase to form a new BSCF + LC composite cathode for IT-SOFCs. LC oxide has negligible oxygen ionic conductivity as compared to BSCF at reduced temperatures, so the introduction of LC would then decrease the overall oxygen ionic conductivity. However, a volume percent of ~28–36% is usually required for the formation of a percolating LC phase [25], therefore, throughout this study 30 vol.% LC, otherwise mentioned, was applied in BSCF + LC composite oxide.

The BSCF + LC composite oxide was prepared and the optimum firing temperature of the cathode layer was investigated by X-ray diffraction (XRD), electrical conductivity, cell performance, environmental scanning electron microscopy (ESEM) and energy dispersive X-ray (EDX), and AC impedance measurements.

2. Experimental

2.1. Cathode powder preparation

Phase-pure BSCF and LC oxide powders were synthesized by a sol–gel method in which the appropriate amounts of metal nitrates served as the metal sources and a combination of EDTA and citric acid as the complexing agents [36]. Mild heating under stirring, induced the gelation of the mixed solution. The resulting gels were pre-treated at 250 °C for 12 h to remove the organics, and then calcined under stagnant air at 900 °C for 5 h to obtain the final products.

2.2. Fuel-cell fabrication

A symmetrical cell with the configuration of: electrode|SDC|electrode was used for the impedance studies. Dense SDC pellets of 12 mm in diameter and 0.8 mm in thickness were prepared by dry pressing and sintered under air at 1350 °C for 5 h. To prepare the composite electrode, the BSCF and LC oxide powders with the volume ratio of 70:30 were first dispersed in a pre-mixed solution of glycerol, ethylene glycol and isopropyl alcohol to form a colloidal suspension by high-energy ball milling (Fritsch Pulverisettle 6) at the rotation rate of 400 rpm for 0.5 h. The obtained slurry was painted symmetrically on both surfaces of the SDC pellet, followed by calcined at 950–1100 °C for 5 h under stagnant air. The cathodes were named, for example, as BSCF + LC30-950, which means the cathode was consisted of 70 vol.% BSCF and 30 vol.% LC and fired at 950 °C. The silver paste was painted onto the electrode surface as the current collector.

Anode-supported cells with SDC as electrolyte were prepared using a co-pressing technique. Anode powders consisted of 60 wt.% NiO and 40 wt.% SDC were prepared by mixing NiO and SDC in an agate mortar. To fabricate the single cell, the well-mixed NiO-SDC powder was firstly pressed as a substrate, SDC powder was then added onto the substrate and pressed again to form a bi-layer pellet. The bi-layer pellets were then fired under stagnant air at 1350 °C for 5 h for the densification of the electrolyte layer. The BSCF + LC based slurry was painted onto the central surface of the electrolyte and fired at 950 or 1000 °C for 2 h under air. The resulting coin-shape cathode had a thickness of 10–20 μm and an effective area of 0.72 cm^2.

2.3. Single cell test

I–V polarization curves were collected using a Keithley 2420 source meter based on the four-probe configuration. Three percent H_2O humidified H_2 at a flow rate of 80 ml min^{-1} (STP) was fed into the anode chamber as fuel and air into the cathode chamber as oxidant gas. Gas flow rates were controlled by mass flow controllers. Ag paste was adopted as the current collector.

2.4. Electrochemical impedance test

The electrode performance was investigated with a symmetrical cell or complete cell configuration by the AC impedance

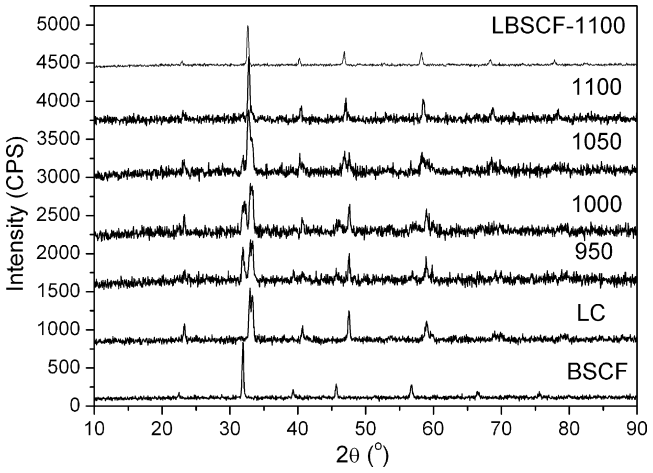

Fig. 1. XRD patterns of BSCF, LC, LBSCF and BSCF + LC calcined at various temperatures.

method using an electrochemical workstation Solartron 1287 potentiostat and a 1260A frequency response analyzer. The frequency range applied was from 0.01 Hz to 10 kHz with a signal amplitude of 10 mV under open cell voltage (OCV) conditions. The overall impedance data were fitted by a complex non-linear least square (CNLS) fitting program in ZView 2.9b software.

2.5. Other characterizations

X-ray diffraction (XRD, Bruker D8 Advance) patterns were used to analyze the chemical compatibilities against high temperature. The microscopic features of the prepared electrodes were characterized using an Environmental Scanning Electron Microscopy (ESEM, QUANTA-2000) equipped with an energy dispersive X-ray (EDX) attachment. The specific surface areas of the samples were characterized by N_2 adsorption using a BELSORP II instrument at the temperature of liquid nitrogen. Electrical conductivity was measured by the four-probe DC technique, using Ag paste as electrodes. The current and the voltage were detected by the Keithley 2420 source meter at intervals of 5 °C over a temperature range of 300–900 °C.

3. Results and discussion

Cobalt-based perovskites usually have a high reactivity. The solid-state reaction between LC and BSCF phases was first investigated. As shown in Fig. 1, pure-phase BSCF and LC oxides had a cubic and a rhombohedral perovskite structure, respectively. After calcination at 950 °C for 5 h under air, the BSCF + LC composite oxide still displayed mainly a physical mixture of the LC and BSCF oxides, based on the XRD results. This suggests that a solid-state reaction between BSCF and LC phases was relatively weak at 950 °C. With increase of calcination temperature to 1000 °C, the diffraction peak (around 32°) of BSCF at mirror index (1 1 0) was significantly broadened as compared to fresh BSCF, and the two diffraction peaks at mirror index of (1 1 0) and (1 0 4) for the rhombohedral perovskite structure of LC merged into one broad peak. This suggests that a certain degree of reaction might have happened between the BSCF and LC phases at 1000 °C. The solid-state reaction is usually via the inter-diffusion between the adjacent two phases. At a calcination temperature of 1000 °C, the inter-diffusion should be limited and a compositional gradient across the interface is likely built, which may be the cause of the broadening of the diffraction peaks for the BSCF and LC. With further increase in the calcination temperature to 1050 °C, the peak intensity of the BSCF and LC phases was significantly reduced, while a new cubic perovskite phase with a lattice constant of $a = 3.879$ Å was formed. When the calcination temperature was 1100 °C, the BSCF and LC phases totally disappeared, and the final product was composed only of the new perovskite-structured oxide with $a = 3.879$ Å. It is well known that perovskite structure is flexible enough to adopt a wide range of metal ions in its A and B sites. Based on their ionic radius sizes, La^{3+}, Ba^{2+} and Sr^{2+} occupied the A-site of the perovskite while cobalt and iron ions occupied the B-site. Because of the unit for the mole ratio of (La, Ba, Sr) to (Co, Fe) in BSCF + LC composite, the complete reaction between BSCF (70 vol.%) and LC (30 vol.%) was likely to form a perovskite with the final composition of $La_{0.316}Ba_{0.342}Sr_{0.342}Co_{0.863}Fe_{0.137}O_{3-\delta}$ (LBSCF). This assumption was indicated by the SEM-EDX examination of the 1100 °C calcined composite oxide, and also supported by the successful synthesis of a pure phase perovskite with the target composition of LBSCF.

The surface morphologies and micro-composition of BSCF, LC and BSCF + LC composite oxide calcined at various temperatures are shown in Fig. 2 and the corresponding EDX results are listed in Table 1. BSCF had a primary particle size of 1–2 μm (Fig. 2A), much larger than that of LC, which is 100–200 nm (Fig. 2B). A BET surface area measurement shows that BSCF had a low surface area of 0.25 $m^2\ g^{-1}$, as compared to 4.0 $m^2\ g^{-1}$ for LC. Fig. 2C demonstrates that the physically mixed BSCF + LC composite oxide is characterized by the fine LC particles surrounding the surface of a BSCF large particle. For the BSCF + LC composite oxide calcined at 950 or 1000 °C for 5 h, their morphologies did not change signifi-

Table 1
EDX results for BSCF + LC composite calcined at various temperatures

T (°C)	Metal elements in fine particles (at%)					Metal elements in coarse particles (at%)				
	Sr	Ba	La	Fe	Co	Sr	Ba	La	Fe	Co
950	4.69	5.02	14.2	2.46	22.32	9.13	8.72	3.83	3.74	18.92
1000	7.52	8.42	12.6	3.73	26.68	8.24	7.98	5.57	3.66	15.52
1050	7.01	6.15	7.07	2.87	16.14	9.15	8.77	6.85	3.44	16.95
1100	–	–	–	–	–	9.13	8.68	8.38	4.14	21.92

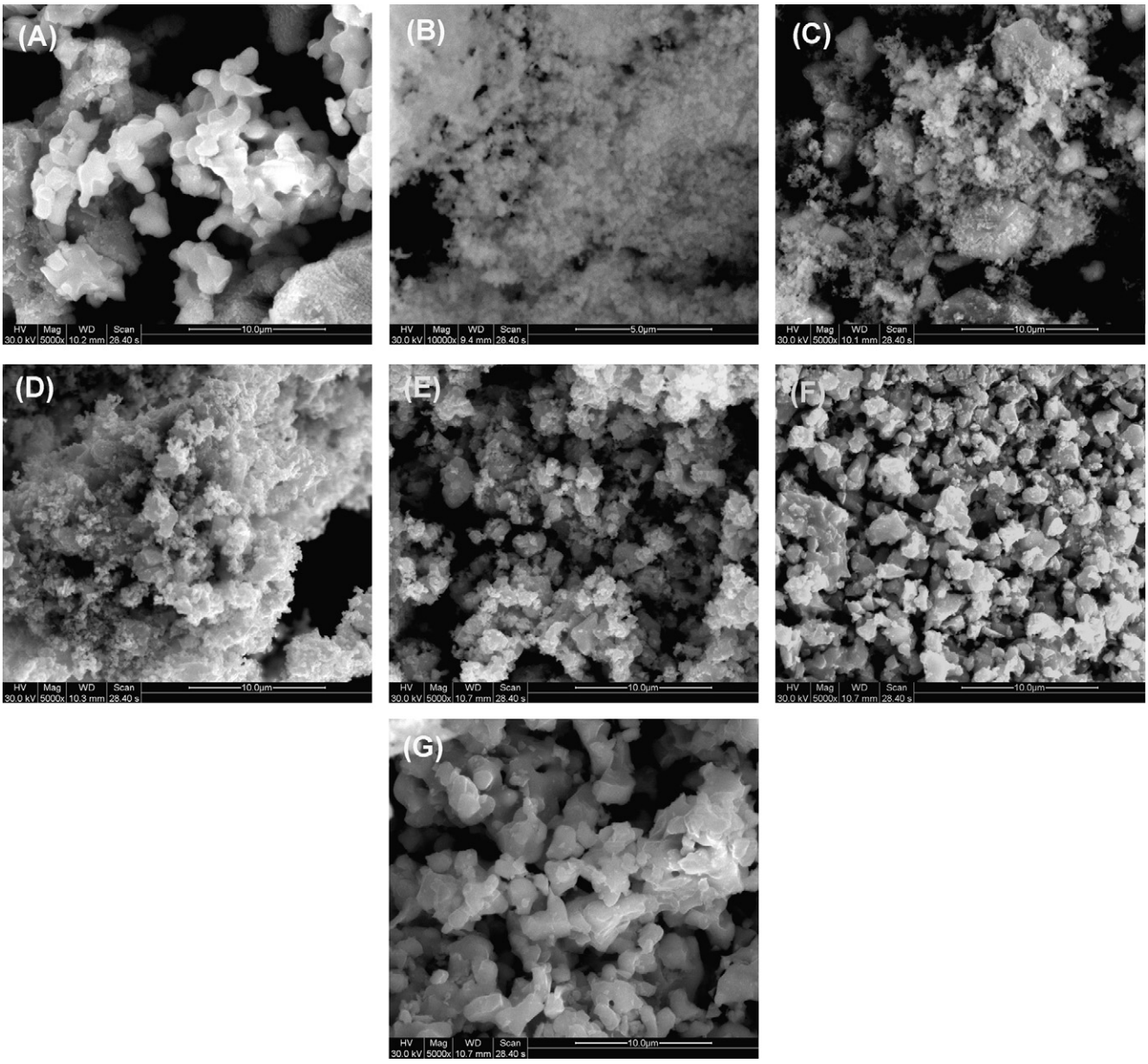

Fig. 2. SEM images of the BSCF (A), LC (B), BSCF + LC mixture (C) and BSCF + LC calcined at 950 °C (D), 1000 °C (E), 1050 °C (F) and 1100 °C (G).

cantly from the fresh one; however, the attachment of LC to the BSCF surface was obviously improved. The EDX results of the 950 °C calcined sample demonstrated that the fine particles were mainly composed of La and Co and oxygen. However, small concentrations of Ba, Sr and Fe elements were also detected demonstrating the inter-diffusion of BSCF into the lattice structure of LC. The big particles were mainly composed of Ba, Sr, Co, Fe and O. However, La was also detected in those particles demonstrating the diffusion of LC into the BSCF lattice. For the 1050 °C calcined sample, the amount of the large-size grains decreased substantially. EDX examination showed that the compositional difference of the different zones was decreased as compared to the lower temperature calcined samples (950 and 1000 °C). However, some BSCF-enriched and LC-enriched zones were still detected. For the 1100 °C calcined sample, all the zones showed the homogeneous composition of LBSCF within the experimental error, which indicates the complete reaction between BSCF and LC.

The electrical conductivities of BSCF, LC and BSCF + LC composite oxide calcined at various temperatures for 5 h under air, are shown in Fig. 3. Due to the reaction between BSCF and LC at high temperature, we were not able to obtain a dense sintering body of the composite oxide. The measured porosity of the sintering bar for BSCF + LC composite oxide at 950, 1000 and 1050 °C was 13.1%, 12.0% and 14.3%, respectively. The conductivity of BSCF + LC composite reported here was the adjusted value by taking account of the porosity. LC reached a maximum conductivity of ~685 S cm^{-1} at around 450 °C, similar to that reported by Mineshige et al. for a high temperature quenched LC sample [37], but smaller than that reported by Petrov et al. [38]. BSCF + LC composite oxide had an obviously improved electrical conductivity as compared to the single

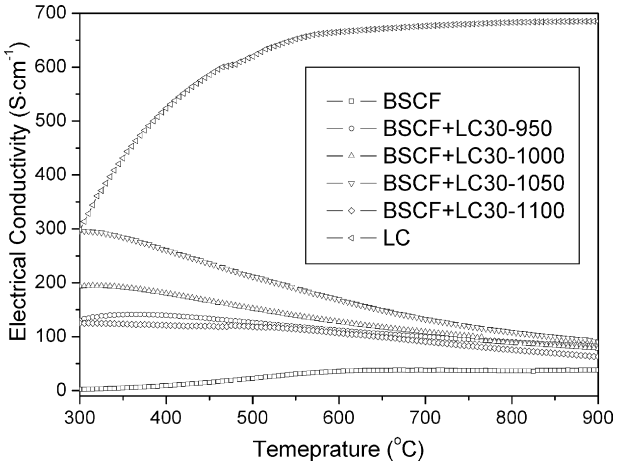

Fig. 3. The electrical conductivities of BSCF, LC and BSCF + LC composite calcined at various temperatures for 5 h under air.

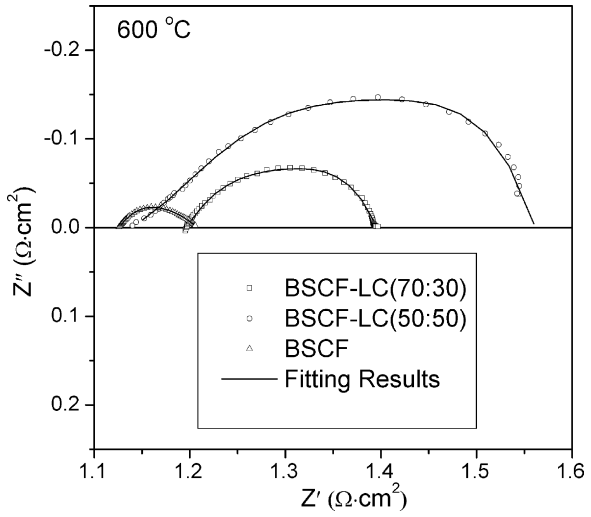

Fig. 4. Nyquist plots of EIS for BSCF, BSCF (70 vol.%) + LC (30 vol.%) and BSCF (50 vol.%) + LC (50 vol.%) at 600 °C.

BSCF oxide, especially at lower operating temperatures. The higher the calcination temperature of the BSCF + LC composite oxide, the higher the conductivity showed. A maximum conductivity of ~300 S cm^{-1} at the operating temperature of ~300 °C for BSCF-LC30-1050 was observed. For the BSCF-LC30-950 and BSCF-LC30-1000, the conductivities increased firstly with the increase of operating temperature, reached a maximum at an operating temperature of ~365 and ~305 °C, respectively, and then decreased with the further increase of operating temperature. While for BSCF-LC30-1050, the conductivity monotonically decreased with the increase of operating temperature. The conductivity of composite oxide is closely related with the mixing state and the possible reaction between the two phases. It was reported that the electrical conductivity for $La_{1-x}Sr_xCoO_{3-\delta}$ (LSC) increased with the increase of Sr doping concentration at $x < 0.4$ [38]. The reaction between BSCF and LC led to the incorporation of Ba^{2+}/Sr^{2+} into the structure of LC, therefore, resulting in the increase of the conductivity of the LC phase. The diffusion of LC into BSCF also increased the conductivity of BSCF phase, as supported by the higher conductivity of $La_{0.3}Ba_{0.35}Sr_{0.35}Co_{0.86}Fe_{0.14}O_{3-\delta}$ (LBSCF) than BSCF from Fig. 3. With the increase of the calcination temperature, the solid-state reaction between BSCF and LC phases increased, therefore, an increase of the electrical conductivity was observed for BSCF + LC composite oxide. The temperature dependence of the conductivity for LSC was found to change from first increase and then decrease with temperature at low Sr^{2+} concentration in LSC, and then to monotonically decrease with temperature at $x \geq 0.25$ ($La_{1-x}Sr_xCoO_{3-\delta}$) [37]. Because of the much higher electronic conductivity of LC than BSCF, the electrical conductivity of the composite oxide was contributed more significantly from the LC phase. With the increase of calcination temperature, more significant diffusion of BSCF into LC phase occured, and explained the observed phenomena of increased conductivity of the BSCF + LC composite oxide with increase of calcination temperature. The decreased conductivity for LBSCF as compared to the composite oxide calcined at 1050 °C and was likely caused by excessive Sr doping and the blocking effect of Ba^{2+} to the ambipolar transporting of electrons.

The cathode performance for the BSCF, LC and BSCF + LC composite oxide calcined at 950 °C was then investigated by the AC impedance spectroscopy based on a symmetrical cell configuration under asymmetric air atmosphere. The Nyquist plots of the electrochemical impedance spectra (EIS) for BSCF, BSCF-LC30-950 and BSCF-LC50-950 at 600 °C are shown in Fig. 4. As discussed by previous workers [30], the high-frequency intercept of the impedance spectrum gives the ohmic resistance of the cell (R_{ohm}), which includes the resistive contributions of the electrolyte, the two electrodes, the current collectors and the lead wires. In this study, the ohmic resistance of the two electrodes, the current collectors and the lead wires was reasonably considered to be negligible. The low-frequency intercept gives the total resistance ($R_{ohm} + R_p$), which includes the ohmic resistance of the cell, concentration polarization (mass-transfer or gas-diffusion polarization) resistance and the effective interfacial polarization resistance associated with the electrochemical reactions at the electrode-electrolyte interface. The ohmic resistance (R_{ohm}) and the total interfacial polarization resistance of the cell were extracted by fitting the impedance spectra to an equivalent circuit with a configuration of $R_{ohm}(R\text{-CPE})_{HF}(R\text{-CPE})_{LF}$. The simulation data are shown in Table 2. The resistance at the high frequency may reflect the charge transfer (R_1), and the lower frequency arc of the oxygen dissociation and bulk or surface oxygen diffusion process (R_2). An increase in both the charge transfer polarization resistance and the oxygen dissociation/surface oxygen diffusion polarization resistance was

Table 2
Results of fitting EIS of BSCF and BSCF + LC composite cathodes measured at 600 °C

Electrode	R_{ohm}	R_1	CPE_1		R_2	CPE_2	
			T_1	P_1		T_2	P_2
BSCF	1.126	0.008	5.772	0.971	0.064	0.129	0.744
BSCF-LC50-950	1.201	0.029	0.021	0.905	0.169	0.048	0.847
BSCF-LC50-1000	1.143	0.087	0.104	0.650	0.335	0.070	0.881

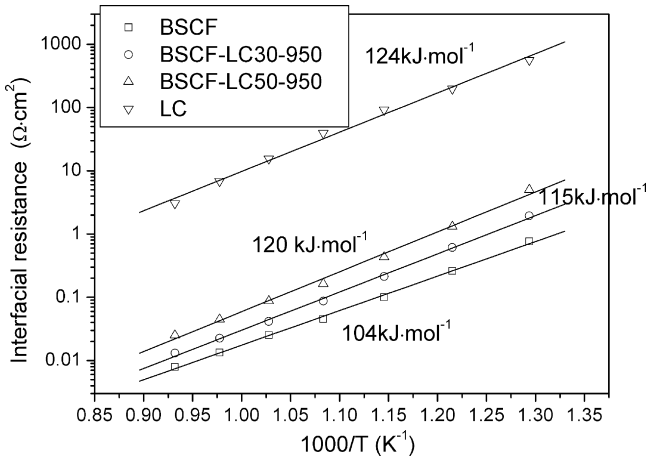

Fig. 5. Arrhenius plots of ASRs for BSCF, LC and BSCF + LC (70:30) and BSCF + LC (50:50) cathodes calcined at 950 °C.

observed with the increase of LC doping concentration, coincided with the fact of worse cathode performance of LC than BSCF. The temperature dependence of the area specific resistances (ASRs) of BSCF, SCF-LC30-950 and SCF-LC50-950 are shown in Fig. 5. As compared to the pure BSCF cathode, the performance of the BSCF + LC composite cathode decreased slightly. As a whole, BSCF + LC composite cathode still displayed very promising results, for example, an ASR as low as 0.21 and 0.43 Ω cm^2 was obtained (at 600 °C) for the 30 and 50 vol.% LC contained BSCF + LC composite cathodes calcined at 950 °C for 5 h, respectively.

Based on the XRD results, the calcination temperature had significant effect on the phase reaction between LC and BSCF. The influence of calcination temperature on the cathode performance of BSCF-LC30 oxide was then investigated, and the results are shown in Fig. 6. It was found that the 950 and 1000 °C calcined samples showed the similar cathode performance, while the increase of calcination temperature from 1000 to 1050 °C resulted in the slight increase of the ASRs. The further increase of calcination temperature to 1100 °C resulted in the sharp increase of the ASRs. Based on the results in Figs. 1 and 2, the phase reaction at calcination temperature of 950 and 1000 °C was only limited. The inter-diffusion of BSCF and LC resulted in the limited incorporation of LC and BSCF to each other. The incorporation of BSCF into LC resulted in an increase of the oxygen reduction properties of LC due to the creation of oxygen vacancy in the LC lattice and also the increase of overall electrical conductivity of the cathode, while the incorporation of LC into BSCF resulted in the decrease oxygen reduction activity of BSCF. The best calcination temperature would be an overall balance for the performance of the BSCF and LC phases in the BSCF + LC composite, which should be around 950–1000 °C in this study. For a calcination temperature of 1050 °C or higher, however, the reaction between BSCF and LC was so seriously, the deterioration of the performance for the BSCF phase was more significantly than the improvement from the LC phase, therefore, a decrease in overall cathode performance was observed.

Therefore, the calcination temperature of 950 and 1000 °C was then selected for the fabrication of whole cells for *I–V* polarization study. Complete fuel cells of Ni + SDC anode supported thin-film SDC electrolyte (~30 μm) with BSCF-LC30 composite oxide as cathode was built. *I–V* curves for the cells using 3% water humidified hydrogen was tested and the results are shown

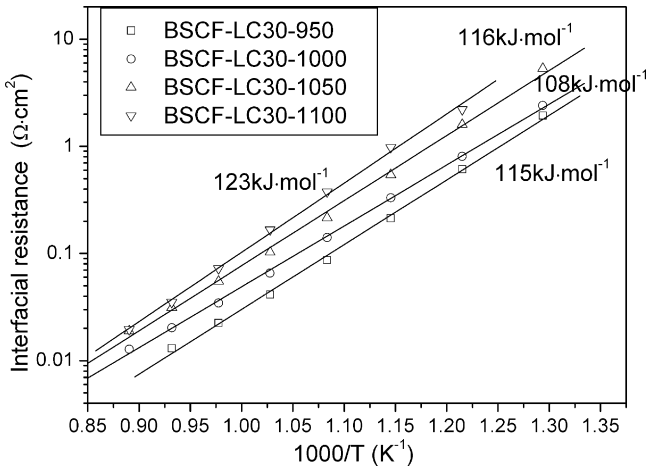

Fig. 6. Arrhenius plots of ASRs for BSCF + LC composite cathodes calcined at various temperatures.

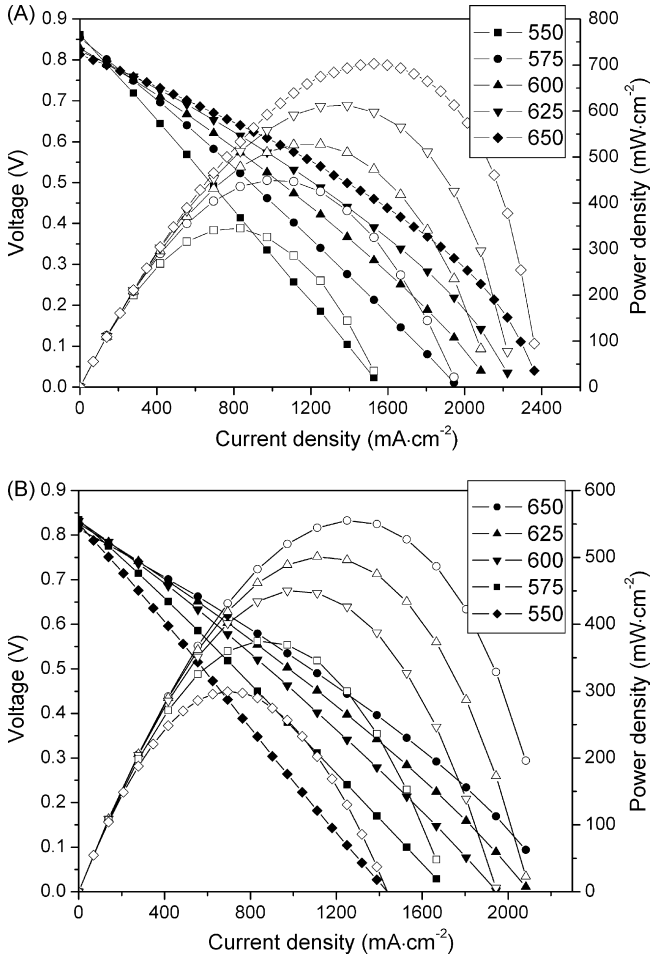

Fig. 7. *I–V* and *I–W* curves of the single cells with the cathodes fired at 950 °C (A) and 1000 °C (B).

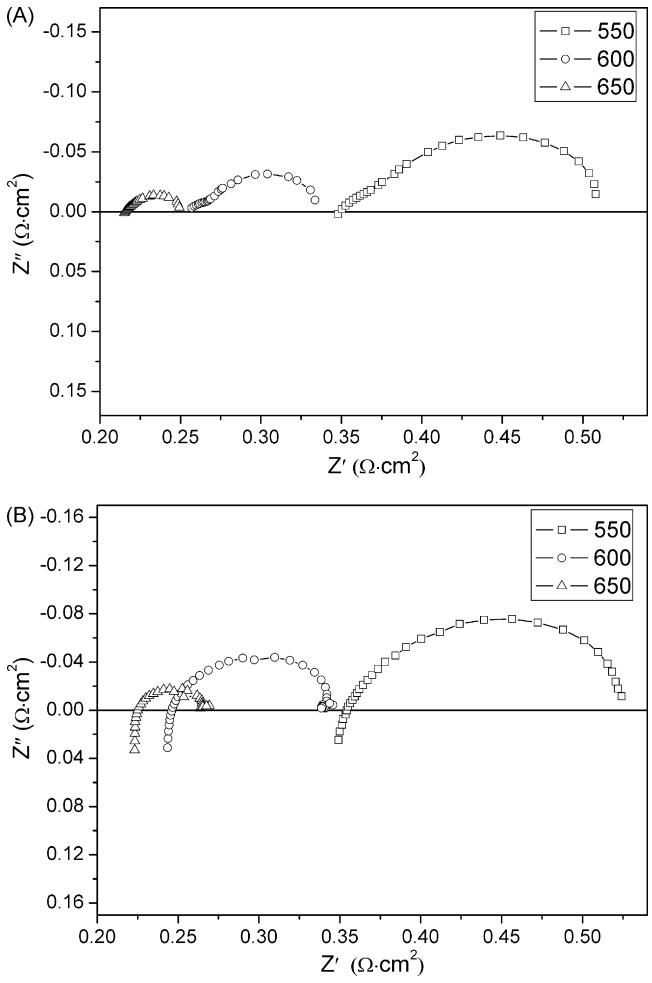

Fig. 8. Impedance spectra for single cells with BSCF + LC composite cathodes fired at 950 °C (A) and 1000 °C (B).

in Fig. 7. Both fuel cells displayed attractive performances. A peak power density as high as ~700 mW cm^{-2} at 650 °C, and ~525 mW cm^{-2} at 600 °C was achieved for the 950 °C calcined one. At higher operating temperatures, the fuel cell with the 950 °C calcined cathode shows slightly better performance than the 1000 °C calcined one. While at a low operating temperature, such difference was negligible. The corresponding EIS are shown in Fig. 8. The electrode polarization resistance from the EIS shown here are included for both the anode and cathode polarizations. Even at a low operating temperature of 550 °C, the ohmic resistance still dominated the cell resistance both for the 950 and 1000 °C calcined samples. Therefore, a reduction of the electrolyte resistance by further reducing the electrolyte thickness or increasing the electrolyte conductivity with improved preparation techniques or increasing the raw material purity would substantially increase of the fuel cell performance.

4. Conclusion

A new BSCF + LC composite cathode is reported for potential application in IT-SOFCs. LC oxide was added as a high electrically conducting phase to improve the performance of the BSCF cathode. A solid-state reaction between LC and BSCF was observed above 950 °C. A new phase with the composition of $La_{0.316}Ba_{0.342}Sr_{0.342}Co_{0.863}Fe_{0.137}O_{3-\delta}$ with a lattice parameter of 3.789 Å was formed at 1100 °C. The inter diffusion between the BSCF and LC phases was identified by the SEM-EDX results. The electrical conductivity of BSCF + LC increased with the increase of the calcination temperature and reached a maximum of ~300 S cm^{-1} at 1050 °C. The improved conductivity resulted in attractive cathode performance for IT-SOFCs. An ASR as low as 0.21 Ω cm^2 was obtained at 600 °C for the 30 vol.% LC contained BSCF + LC composite cathode calcined at 950 °C for 5 h (BSCF-LC30-950). A peak power density as high as ~700 mW cm^{-2} at 650 °C, and ~525 mW cm^{-2} at 600 °C was achieved for a fuel cell with a BSCF-LC30-950 cathode. All the above results suggest a potential application of the BSCF + LC composite oxide as the cathode in IT-SOFCs.

Acknowledgements

This work was supported by the National Natural Science Foundation of China, under contracts No. 20646002 and No. 20676061, and also Natural Science Foundation of JiangSu Province under contract No. BK2006180. Dr. Zongping Shao also acknowledges the set-up funding from Nanjing University of Technology.

References

[1] B.C.H. Steele, A. Heinzel, Nature 414 (2001) 345.
[2] S.C. Singhal, K. Kendall, High Temperature Solid Oxide Fuel Cells: Fundamentals, Design and Applications, Elsevier Advanced Technology, UK, 2003.
[3] D. Dulieu, et al., in: P. Stevens (Ed.), 3rd European SOFC Forum, European Fuel Cell Forum, Oberrohrdorf, Switzerland, 1998, pp. 447–458.
[4] C. Lara, M.J. Pascual, R. Keding, A. Durán, J. Power Sources 157 (2006) 377.
[5] T. Kenjo, M. Nishiya, Solid State Ionics 57 (1992) 295.
[6] M.J.L. Ostergard, C. Clausen, C. Bagger, M. Mogensen, Electrochim. Acta 40 (1994) 1971.
[7] K. Sasaki, I.P. Wurth, M. Godickemeier, A. Mitterdorfer, L.J. Gauckler, in: M. Dokiya, O. Yamamoto, H. Tagawa, S.C. Singhal (Eds.), Proceedings of the Fourth International Symposium on Solid Oxide Fuel Cells, The Electrochemical Society, Pegton, NJ, 1995, p. 625.
[8] P. Holtappels, C. Bagger, J. Eur. Ceram. Soc. 22 (2002) 41.
[9] E.P. Murray, S.A. Barnett, Solid State Ionics 143 (2001) 265.
[10] B.C.H. Steele, Solid State Ionics 129 (2000) 95.
[11] R. Doshi, V.L. Richards, J.D. Carter, X. Wang, M. Krumpelt, J. Electrochem. Soc. 146 (1999) 1273.
[12] Y. Jiang, S.Z. Wang, Y.H. Zhang, J.W. Yan, W.Z. Li, J. Electrochem. Soc. 145 (1998) 373.
[13] C.R. Xia, W. Rauch, F.L. Chen, M.L. Liu, Solid State Ionics 149 (2002) 11.
[14] M.J. Jorgensen, S. Primdahl, M. Mogensen, Electrochim. Acta 44 (1999) 4195.
[15] M.J.L. Ostergard, C. Clausen, C. Bagger, M. Mogensen, Electrochim. Acta 40 (1995) 1971.
[16] Z. Lei, Q. Zhu, L. Zhao, J. Power Sources 161 (2006) 1169.
[17] T. Tsai, S.A. Barnett, Solid State Ionics 93 (1997) 207.
[18] M. Nagata, C. Iwasawa, Y. Seino, Proceedings of the 2nd International Fuel Cell Conference, Kobe, Japan, 1996, p. 255.
[19] S.P. Jiang, W. Wang, J. Electrochem. Soc. 152 (2005) A1398.
[20] X.D. Zhu, K.N. Sun, N.Q. Zhang, X.B. Chen, L.J. Wu, D.C. Jia, Electrochem. Commun. 9 (2007) 431.
[21] C.R. Xia, M.L. Liu, J. Am. Ceram. Soc. 84 (8) (2001) 1903.

[22] C.R. Xia, F.L. Chen, M.L. Liu, Electrochem. Solid-State Lett. 4 (5) (2001) A52.
[23] C.R. Xia, M.L. Liu, Solid State Ionics 144 (2001) 249.
[24] X. Zhang, M. Robertson, S. Yick, C. Deĉes-Petit, E. Styles, W. Qu, Y. Xie, R. Hui, J. Roller, O. Kesler, R. Maric, D. Ghosh, J. Power Sources 160 (2006) 1211.
[25] V. Dusastre, J.A. Kilner, Solid State Ionics 126 (1999) 163.
[26] Z. Shao, S.M. Haile, Nature 431 (2004) 170.
[27] S. Lee, Y. Lim, E.A. Lee, H.J. Hwang, J.-W. Moon, J. Power Sources 157 (2006) 848.
[28] Z. Duan, M. Yang, A. Yan, Z. Hou, Y. Dong, Y. Chong, M. Cheng, W. Yang, J. Power Sources 160 (2006) 57.
[29] J. Peña-Martínez, D. Marrero-López, J.C. Ruiz-Morales, B.E. Buergler, P. Núñez, L.J. Gauckler, Solid State Ionics 177 (2006) 2143.
[30] Q.L. Liu, K.A. Khor, S.H. Chan, J. Power Sources 161 (2006) 123.
[31] B. Wei, Z. Lü, X. Huang, S. Li, G. Ai, Z. Liu, W. Su, Mater. Lett. 60 (2006) 3642.
[32] S. McIntosh, J.F. Vente, W.G. Haije, D.H.A. Blank, H.J.M. Bouwmeester, Chem. Mater. 18 (2006) 2187.
[33] Y. Wang, S. Wang, Z. Wang, T. Wen, Z. Wen, J. Alloys Compd. 428 (2007) 286.
[34] H.J. Hwang, J.-W. Moonb, S. Lee, E.A. Lee, J. Power Sources 145 (2005) 243.
[35] V.V. Kharton, F.M. Figueiredo, A.V. Kovalevsky, A.P. Viskup, E.N. Naumovich, A.A. Yaremchenko, I.A. Bashmakov, F.M.B. Marques, J. Eur. Ceram. Soc. 21 (2001) 2301.
[36] W. Zhou, Z. Shao, W. Jin, J. Alloys Compd. 426 (2006) 368.
[37] A. Mineshige, M. Inaba, T. Yao, Z. Ogumi, J. Solid State Chem. 121 (1996) 423.
[38] A.N. Petrov, O.F. Kononchuk, A.V. Andreev, V.A. Cherepanov, P. Kofstad, Solid State Ionics 80 (1995) 189.